Analytical models to estimate the structural behaviour of fused deposition modelling components

emerald PUBLISHING

Rapid Prototyping J

Analytical models to estimate the structural behaviour of Fused Deposition Modelling components

Journal:	*Rapid Prototyping Journal*
Manuscript ID	RPJ-07-2020-0145.R1
Manuscript Type:	Original Article
Keywords:	Material Extrusion, Fused Deposition Modelling (FDM), structural properties, analytical models, prediction performance

Analytical models to estimate the structural behaviour of Fused Deposition Modelling components

Purpose – Evaluate the capability and performance of analytical models to predict the structural mechanical behaviour of parts fabricated by Fused Deposition Modelling (FDM).

Design/methodology/approach – A total of eight existing and newly proposed analytical models, tailored to satisfy the structural behaviour of FDM parts, are evaluated in terms of their capability to predict the Ultimate Tensile Stress (UTS) and the Elastic Modulus (E) of parts made of PLA (Polylactic acid) by the FDM process. This evaluation is made by comparing the structural properties predicted by these models with the experimental results obtained from tensile tests on FDM specimens fabricated with variable infill percentage, perimeter layers and build orientation.

Findings – Some analytical models are able to predict with high accuracy (prediction errors smaller than 5%) the structural behaviour of FDM and categories of similar additive manufactured parts. The most accurate model is the Gibson's & Ashby, followed by the efficiency model and the two new proposed exponential and variant Duckworth models.

Research limitations/implications – The study has been limited to uniaxial loading conditions along three different build orientations.

Practical implications – The structural properties of FDM parts can be predicted by analytical models based on the process parameters and material properties. Product engineers can use these models during the design for additive manufacturing (DfAM) process.

Originality / Value – Existing methods to estimate the structural properties of FDM parts are based on experimental tests; however, such methods are time consuming and costly. In

this work the use of analytical models to predict the structural properties of FDM parts is proposed and evaluated.

Keywords: Material Extrusion; Fused Deposition Modelling (FDM); structural properties; analytical models; prediction performance.

1. Introduction

Additive manufacturing (AM) technologies are becoming very popular to produce end-use parts due to their several advantages such as fast production cycles, high complexity and personalized parts (Domingo-Espin, *et al*., 2015), and the production of a large range of prototypes or functional components with complex geometries, such as those obtained from a topology optimization process (Chacón *et al*., 2017). Fused Deposition Modelling (FDM) is one of the most widely used AM techniques because of the wide range of commercially available systems and materials, whose costs range from very low to high. In the FDM process, parts are built layer by layer by heating a thermoplastic filament, usually acrylonitrile butadiene styrene (ABS) or polylactic acid (PLA), to a semi-liquid state in order to be extruded through a moving nozzle on the X-Y plane and deposited on a platform that moves along the Z direction. The FDM process parameters can be classified into two main groups (Cuan-Urquizo *et al*., 2019): 1) manufacturing parameters and 2) structural parameters. The first group comprises the extrusion temperature, build platform temperature, extrusion rate, nozzle transverse speed, layer time, etc. The second group includes the infill density, rasters angle, part/build orientation, stacking sequence, etc.

Although the FDM process is relatively simple, it has some technical issues that must be considered when designing parts for FDM. One major issue is that the mechanical properties

of FDM parts are still uncertain because they are orthotropic, depend on the process parameters, and differ from the properties of the unprocessed (filament) material (Alafaghani *et al.*, 2017). To overcome this major issue many research works have focused on studying the mechanical behaviour of FDM parts and optimizing the process parameters. However, most of these works use experimental and numerical approaches, and very few have considered the development and use of analytical models. The lack of structural predictive models leads to uncertainties when selecting the process parameters; and consequently, the mechanical properties of the resultant FDM parts are uncertain. In addition, this lack of analytical models have limited the use of AM processes in the fabrication of end-use parts and the evolution of design for additive manufacturing (DfAM) techniques.

The aim of this paper is to tailor and assess existing and newly proposed analytical models to predict the structural performance of FDM components. These models use the infill percentage, part orientation and material properties process parameters to estimate the structural behaviour of FDM parts. The evaluation is based on a comparative analysis with experimental results in order to determine their prediction performance.

2. Literature review

2.1 Experimental studies

Anh *et al*. (2002) investigated the effects of several process parameters on the tensile and compressive strength of ABS-FDM. They concluded that the air gap and raster orientation greatly affect the tensile strength, which showed anisotropic characteristics. The compressive strength was found to be greater than the tensile strength. Ang *et al.* (2006) conducted a similar study using samples of ABS scaffold structures. It was found that the air gap and raster width are the most significant parameters that affect the porosity and mechanical

properties. In addition, it was observed that the relationship between the mechanical properties and porosity is logarithmic.

On the other hand, Rayegani and Onwubolu (2014) presented an investigation to determine the relationship among the FDM process parameters and the tensile strength of ABS parts. The part orientation, raster angle, raster width and air gap process parameters were considered. A hybrid Group Method for Data Handling (GMDH) tensile strength model was also developed. It was concluded that the part orientation and raster angle affect the tensile strength, and the GMDH modelling system is able to properly predict the tensile strength behaviour. Similarly, Sealy *et al*. (2017) investigated the influence of layer thickness, raster angle, shell layers and applied shot peening on the tensile strength of BS-FDM parts. It was observed that shot peening had a significant effect on decreasing the tensile strength. On the other hand, Sukindar *et al.* (2017) reported the impact of layer thickness, shell thickness and printing speed on the tensile strength of PLA-FDM samples. The results showed that the shell thickness has the most significant impact on the tensile strength.

More recently, Vanaei H. *et al.* (2020) presented an experimental investigation about the influence of various process parameters on the thermal and mechanical properties of PLA-FDM parts. The results showed that the extruder temperature has a more significant influence than the other parameters. Likewise, Cerda-Avila *et al.* (2020) presented a large set of experimental results to analyse the structural behaviour of PLA-FDM parts with variable process parameters. A new experimental methodology based on the normalization of the structural properties was also proposed. The results showed that the infill and the build orientation process parameters have a large influence on the resultant Ultimate Tensile Stress (UTS) and the elastic modulus (E).

2.2 Numerical models

Some research works have used numerical models to analyse and evaluate the mechanical performance of parts manufactured by FDM. Zhang and Chou (2006) proposed a thermo-mechanical Finite Element Method (FEM) model to simulate the filament deposition. The results showed that a short-raster tool path leads to a higher residual stresses compared to long-raster and alternate-raster patterns, despite both have similar stress distributions and distortion features. On the other hand, Hambali *et al.* (2010) presented three FEM models of a bracket with three different build orientations and one loading condition. Experimental tests of the brackets were conducted and the results showed a non-linear trend while the FEM results followed a linear behaviour. This indicates that a nonlinear and dynamic FEM model may be more suitable. Likewise, Rezayat *et al*. (2015) presented a simplified FEM model of a tensile specimen with different raster angles and air gaps. The results showed that at the filament scale the load transfer mechanism shifted from the rasters to the contour when the air gap was changed from a negative to a positive value. Moreover, it was suggested that the mechanical properties of FDM parts could potentially improve if the raster contour patterns currently used in AM systems were redesigned.

Górski *et al.* (2015) compared a numerical FEM model versus an experimental test. Though the results were very similar under bending conditions, the prediction of internal stresses was inconclusive, and the computational time required was very large. Similarly, Somireddy and Czekanski (2017) presented a FEM model of FDM mesostructured parts. It was concluded that the differences between the numerical and the experimental results are because in the numerical model a perfect bonding among layers and roads is assumed. On the other hand, Somireddy *et al.* (2018) developed FEM models of a Representative Volume Element (RVE) subjected to tensile loading. These models capture the influence of build orientation, printing

direction and layer thickness. It was observed that the material behaviour depends on the build orientation. More recently, Cerda-Avila *et al*. (2019) presented a study to predict the mechanical performance of FDM parts using numerical modelling. Simplified FEM models with variable infill values were analysed and compared with their corresponding experimental results. It was observed that although the numerical and experimental results have the same trends, the numerical models over-predicted the experimental results.

2.3 Predictive models

Predictive models for the mechanical behaviour of FDM parts have been also reported in the literature. Croccolo *et al*. (2013) developed an analytical model for the prediction of the elastic modulus and stiffness based on the bead width and height, raster angle, number of contours and build direction process parameters. The results showed that the proposed model was able to reproduce the rupture event of every single bead, and predict the failure of the whole part. On the other hand, Casavola *et al.* (2016) used the classical laminated theory (CLT) to describe the mechanical behaviour of FDM specimens. Although the model was able to predict with high accuracy the elastic modulus of FDM components made of PLA and ABS, it did not consider process parameters such as the extrusion temperature, feed rate, and vertical building direction.

Regarding optimization, Garg *et al.* (2014) proposed a hybrid M5′-genetic programming (M5′-GP) approach for empirical modelling of the FDM process. The proposed methodology used a GP model in parallel with an M5′ model. The input parameters were the layer thickness, build orientation, raster angle, raster width and air gap, whereas the output parameter was the compressive strength. The results showed that the proposed approach fits better than those support vector regression (SVR) and adaptive neuro fuzzy inference system

(ANFIS) models. On the other hand, Costa *et al*. (2017) proposed an analytical solution to the transient heat conduction phenomenon during filament deposition. It was observed that the predicted and the experimental data for the filament surface temperature showed a good agreement. Recently, Panda *et al*. (2018) presented three numerical methods, genetic programming (GP), automated neural network search (ANS) and response surface regression (RSR), to predict the mechanical properties of honeycomb cellular structures manufactured by FDM. Different cell sizes were experimentally and analytically studied for the prediction of the yield strength and elastic modulus. It was observed that the ANS models performed better than the GP and RSR models. It was also observed that as the cell size increases the yield strength and elastic modulus decrease, whereas as the wall thickness increases the yield strength and elastic modulus increase.

The previous literature review reveals that the influence of the process parameters on the mechanical properties of FDM components has been widely studied in the literature. The results have demonstrated that the air gap, build orientation, layer thickness, infill percentage and number of perimeter layers, are the most significantly influencing process parameters. However, the most of these investigations are based on experimental and numerical approaches, which have shown to be effective but costly and time consuming. Little research work has been made towards the development of analytical models able to predict more efficiently the mechanical properties of FDM parts. Currently, there are no analytical models capable to predict the macro behaviour of the FDM parts from the filament material and process parameters. Thus, the development of such analytical models will not only improve the efficiency of the DfAM process, but also assist engineers in the selection of the process parameters to satisfy the structural needs and existing manufacturing capabilities.

3. Analytical micromechanical models

Since AM is based on adding material to create a component using some particular process parameters such as infill pattern and infill percentage, parts created by AM can be considered as porous. Porous parts are important since they are lighter and reduce the material usage. However, the porosity affects the effective mechanical properties of the part, such as the elastic modulus and load resistance (Ang *et al*., 2006).

Gibson and Ashby (1988) can be considered pioneers in the field of mechanical behaviour of porous materials. Christensen (2000) reported that many materials have an interconnected pore structure where even small pore sizes can form large void volumes, while in large pore sizes the pore phase can be macroscopically interconnected. According to Roberts and Garbozzi (2002), porous materials have a filtration threshold (which may be zero for some models), below which the structure is disconnected. As the threshold is reached, the elastic properties become dependent on small connections, which are increasingly difficult to solve.

Several micromechanical models have been proposed in the literature to determine the homogenized properties of a porous, laminar, composite or heterogeneous material, based on the properties of its constituent materials. Wang and Huang (2018) recently reported a review of these models. From a preliminary analysis of the overall behaviour of several micromechanical models, the following models were selected to evaluate their ability to predict the mechanical behaviour of FDM components.

a) Rule of mixture model

One of the most widely used and simple models is the rule of mixture or Voigt model (Wang and Huang, 2018). This model is expressed as:

$$E_c = E_m V_m + E_p V_p \quad (1)$$

where E_c, E_m and E_p are the elastic modulus of the composite material, the matrix, and the particle respectively; and V_m, V_p are the volume fractions of the matrix and the particle, respectively. In the case of a porous material, such as FDM parts, the particle is considered as a void and therefore E_p is neglected (zero). Thus, Eq. 1 becomes:

$$\frac{E_c}{E_m} = V_m \quad (2)$$

which can be used to estimate the normalized property of porous parts.

b) Efficiency model

A variant of the rule of mixture model or efficiency model has been also used in the literature, and it is represented as (Mouhmid *et al.,* 2006):

$$E_c = \alpha E_m V_m + \beta E_p V_p \quad (3)$$

where α and β are known as the efficiency coefficients, which are determined from experimental data. Similarly, in the case of porous parts, the particle is considered as void and Eq. (3) is reduced to:

$$\frac{E_c}{E_m} = \alpha V_m \quad (4)$$

which represents the normalized property of a porous material.

c) Gibson & Ashby model

One of the most known micromechanical models for porous materials is the Gibson and Ashby model, which is expressed as follows (Gibson and Ashby, 1988):

$$\frac{E_p}{E_0} = C(1-P)^n \quad \text{(for } 0.5 < P < 0.96\text{)} \quad (5)$$

where E_p is the effective elastic modulus of the porous material, E_0 is the elastic modulus of the solid material, P is the porosity, and C and n are the model coefficients, which depend on the micro structure of the material and can be determined from experimental data.

d) Spriggs and Duckworth models

The Duckworth model to determine the effect of porosity on the effective strength of a porous body is (Choren and Heinrich, 2013):

$$\frac{S_p}{S_0} = \exp(-kP) \tag{6}$$

where k is a material-dependent coefficient, P is the porosity, S_p is the UTS of the porous component and S_0 is the UTS of the non-porous material.

Spriggs extended the Duckworth model to the elastic modulus for aluminium oxide with porosities values up to 37%, and presented supporting data for m ranging from 2.7 to 4.3 (Choren and Heinrich, 2013). The Spriggs' model is expressed as:

$$\frac{E_p}{E_0} = \exp(-mP) \tag{7}$$

where m is a material-dependent coefficient, which can be determined from experimental data.

e) Rice model

For porosity values beyond the applicable range of the Spriggs' model, Rice (Choren and Heinrich, 2013) recognized that the role of the pores and matrix materials can be reversed, leading to a theoretical equation applicable to larger values of porosity:

$$\frac{E_p}{E_0} = [1 - \exp(-r\{1 - P\})] \tag{8}$$

where r is a model coefficient that can be determined from experimental data.

f) Hasselman model

Hasselman proposed a modulus-porosity model as follows (Choren and Heinrich, 2013):

$$\frac{E_p}{E_0} = (1 + \left[\frac{AP}{1 - AP - P}\right]) \quad (9)$$

where P is the porosity and A is a model coefficient that can be determined experimentally.

3.1 Proposed models

Two new models to predict the mechanical behaviour of FDM parts are proposed here. These new models were derived from a preliminary analysis of the existing micromechanical models and the FDM experimental data presented in the next section. It was observed that the Duckworth and the Gibson & Ashby models reproduced better the experimental data than the other models. Consequently, these micromechanical models were modified in order to improve their prediction performance. The proposed resulting models are described below.

g) Variant Duckworth model

A variant of the Duckworth model is proposed by adding an efficiency coefficient, resulting in the following hybrid model:

$$\frac{E_p}{E_0} = \beta[exp\ (-mP)] \quad (10)$$

where β is a new proposed efficiency coefficient that can be determined from experimental data, in the same way as the m coefficient.

h) Exponential model

The proposed exponential model considers an exponential behaviour based on the Gibson & Ashby model, but comprising two parameters as follows:

$$\frac{E_p}{E_0} = C(e^{n*(1-P)}) \quad (11)$$

where *C* and *n* are the coefficients of the model, which can be determined from experimental data.

It is important to mention that although the existing and new proposed models described before are defined in terms of the elastic behaviour (i.e. elastic modulus), they can also be used to determine the effective UTS as suggested by Choren and Heinrich, 2013; Gallegos-Nieto *et al.,* 2015; and Hernández-Rivera *et al.,* 2016.

4. Experimental data

To evaluate the prediction performance of the selected micromechanical models when applied to FDM parts, experimental tensile tests were conducted according to the ASTM D638-02a standard (ASTM D638, 2014) and using a Shimadzu AG-100 kN Universal Testing Machine. The tests conditions were: test rate of 5 mm/min, room temperature (~22°C), humidity between 35 to 50% and atmospheric pressure of 827 mbar at 1876 m altitude. The tests specimens were fabricated using the infill values, build orientations and perimeter layers shown in Table 1. The build orientation parameter is represented in Figure 1. In order to have a statistically valid sample, five test specimens were manufactured for each possible combination of the process parameters shown in Table 1. Thus, a total of 396 tensile test specimens were fabricated from PLA filaments in a Creator Pro Flashforge FDM

system and a Creality CR-10S Pro FDM system. Table 2 shows the characteristics of the PLA filaments used in the fabrication of the specimens.

Table 1. FDM process parameters used in the fabrication of the test specimens.

Figure 1. Schematic representation of the build orientation FDM process parameter.

Table 2. Characteristics of the PLA filaments.

In order to provide comparable universal results, independent of the equipment and material used, a normalization process was conducted. This normalization process consisted in dividing the experimental results of each test specimen by the corresponding property of the PLA filament used in the fabrication. The complete set of experimental results has been previously reported and analysed in (Cerda-Avila *et al.*, 2020). Figure 2 shows the normalized results for the UTS and elastic modulus as a function of the infill percentage.

Figure 2. Experimental results for: a) UTS, b) elastic modulus.

5. Models evaluation

The tailoring and evaluation of each micromechanical model was conducted in three steps: 1) calculation of the model's coefficients from the FDM experimental data, 2) estimation of the FDM structural properties using the analytical model and the process parameters values

used in the experimentation, and 3) computation of the model's prediction error according to the following equation:

$$Error = \left(\frac{UTS_{est} - UTS_{exp}}{UTS_{exp}}\right) \times 100\ \% \quad (12)$$

where UTS_{est} is the UTS value estimated by the model and UTS_{exp} is the experimental UTS value. In the case of the elastic modulus prediction, the following equation was used:

$$Error = \left(\frac{E_{est} - E_{exp}}{E_{exp}}\right) \times 100\ \% \quad (13)$$

where E_{est} and E_{exp} are the estimated and experimental values, respectively, of the elastic modulus.

The FDM experimental results were used to calculate the coefficients of each model under analysis. If the model comprises one or two coefficients, one or two experimental points are required, respectively, to calculate those coefficients. Because of the large amount of experimental data available, several coefficient values for each model were calculated and optimized to reduce the overall prediction error at all the experimental points. Moreover, different coefficients were calculated for each build orientation and structural property (UTS and *E*). Notice that the volume fraction value required by some of the models corresponds to the infill FDM process parameter, whereas the porosity value required by some other models corresponds to the complement of the infill value.

5.1 Rule of mixture model

Figure 3 compares the results obtained with the rule of mixture model and the experimental results. It is observed that the rule of mixture model predicts a linear behaviour of the UTS and elastic modulus with respect to the infill percentage of the FDM component, whereas the experimental results suggest a non-linear behaviour. Moreover, the rule of mixture model predicts the same behaviour for all build orientations. In the case of the UTS (Figure 3a), the maximum prediction errors for the flat, on-edge and up-right build orientations are 34%, 35% and 445%, respectively. On other hand, the maximum prediction errors for the elastic modulus (Figure 3b) and the flat, on-edge and up-right build orientations are 51%, 112% and 310%, respectively. These results indicate that in the up-right orientation the adhesion between layers has a very important role in the mechanical properties of the FDM parts, which is not considered by the rule of mixture model.

Figure 3. Results of the rule of mixture model vs. experimental results: a) UTS and b) elastic modulus.

5.2. Efficiency model

Several values of α for the UTS and elastic modulus were calculated by substituting some of the experimental results in Eq. 4. The values of α with best prediction performance for each build orientation (i.e. the minimum prediction error) were selected and are shown in Table 3.

Table 3. Values of the α coefficient.

Figure 4 shows a comparison between the results predicted by the efficiency model and the experimental results. It is observed that although the efficiency model is linear, it predicts

with higher accuracy the experimental results than the rule of mixture model. In the case of the UTS property (Figure 4a), the maximum prediction errors were 15%, 21% and 78% for the flat, on-edge and the up-right build orientation, respectively. Regarding the elastic modulus, (Figure 4b), the analytical and experimental results are very close in the flat orientation (discrepancies smaller than 10%). For the on-edge and the up-right build orientations, the maximum errors were 45% and 87%, respectively. Moreover, the efficiency (α) for the UTS and elastic modulus in the up-right orientation is approximately 33% and 46%, respectively. This reduced structural performance in the up-right orientation is related to the bonding strength among layers rather than to the filament property.

Figure 4. Results of the Efficiency model vs. experimental results: a) UTS and b) elastic modulus.

5.3. Gibson & Ashby model

From the experimental data, all possible combinations of two different experimental points were substituting in Eq. 5 to determine the parameters C and n of the Gibson & Ashby model. Then, the pair of C and n values were optimized to reduce the overall prediction error. Table 4 shows the resultant values for each build orientation and structural property.

Table 4. Values of the C and n coefficients.

Figure 5 presents a comparison of the results predicted by the Gibson & Ashby model and the experimental results. The Gibson & Ashby model shows a distinct exponential behaviour that fits more accurately the experimental data than the linear models. Regarding the UTS

(Figure 5a), the maximum prediction errors are 20%, 23% and 29% for the flat, on-edge and up-right build orientations respectively. In the case of the elastic modulus (Figure 5b), the maximum errors are 9%, 24% and 39% for the flat, on-edge and up-right build orientations, respectively. In the up-right orientation, the model and the experimental results have approximately the same behaviour.

Figure 5. Results of the Gibson & Ashby model vs. experimental results: a) UTS and b) elastic modulus.

5.4. Spriggs and Duckworth models

Several values for the *k* and *m* coefficients of the Duckworth and Spriggs models were calculated from the experimental data and using Eq. 6 and Eq. 7. From these calculations, the values with the best prediction performance for each orientation and mechanical property were selected and are shown in Table 5.

Table 5. Values of the *k* and *m* coefficients.

In Figure 6 the results predicted by the Spriggs and Duckworth models and the experimental results are compared. It is observed that although the models have an exponential behaviour, they poorly match the experimental data. In the case of the Duckworth model, Figure 6a, the maximum error is 139%, whereas the Spriggs model, Figure 6b, has a maximum error of 101%.

Figure 6. Results of the Duckworth and Spriggs models vs. experimental results: a) UTS (Duckworth) and b) elastic modulus (Spriggs).

5.5. Rice model

In the case of the Rice model, several values of the *r* coefficient were computed and optimized to reduce the overall prediction error at the experimental points. The results are shown in Table 6. Figure 7 compares the results predicted by the Rice model and the experimental results. It is observed that the Rice model has an exponential behaviour but with a convex curvature, whilst the experimental data has a concave curvature. In addition, the prediction performance for low infill values (40% to 75%) is greater than for high infill values (85% to 100%). In the case of the UTS (Figure 7a), the maximum prediction errors are 28%, 39%, and 90% for the flat, on-edge and up-right build orientations, respectively. On the other hand, the maximum prediction errors for the elastic modulus (Figure 7b) are 23%, 70%, and 106% for the flat, on-edge and up-right build orientations, respectively.

Table 6. Values of the *r* coefficient.

Figure 7. Results of the Rice model vs. experimental results: a) UTS and b) elastic modulus.

5.6. Hasselman model

In the case of the Hasselman model, several values of *A* (Eq. 9) for each structural property and build orientation were calculated from the experimental results. The *A* values with the best prediction performance were selected and are shown in Table 7.

Table 7. Values of the *A* coefficient.

Figure 8 shows a comparison of the results predicted by the Hasselman model and the experimental results. In the case of the UTS, Figure 8a, the results show that the Hasselman model has a linear behaviour on the flat and on-edge build orientations, and an exponential effect on the up-right orientation. The maximum errors are 17%, 26% and 139% for the flat, on-edge and up-right build orientations, respectively. Regarding the elastic modulus, Figure 8b, the Hasselman model showed a nonlinear behaviour in the three build orientations, and the maximum prediction errors are 32%, 38% and 101% for the flat, on-edge and up-right build orientations, respectively. In addition, the model predicts that for 100% infill the specimens should have the same properties as the raw material (filament), which is not in agreement with the experimental results.

Figure 8. Results of the Hasselman model vs. experimental results: a) UTS and b) elastic modulus.

5.7. Variant Duckworth model

In the case of the variant Duckworth model, Table 8 presents the values of the coefficients β and m obtained from the experimental data. Figure 9 shows a comparison of the results predicted by the Variant Duckworth model and the experimental results. In the case of the UTS, Figure 9a reveals that the proposed model better fits the experimental results than the Duckworth model. The maximum errors are 16%, 29% and 48% for the flat, on-edge and up-right build orientations, respectively. On the other hand, the elastic modulus behaviour predicted by the model (Figure 9b), is less accurate than for the UTS, having maximum

prediction errors of 24%, 55% and 56% for the flat, on-edge and up-right build orientations, respectively.

Table 8. Values of the β and m coefficients.

Figure 9. Results of the Variant Duckworth model vs. experimental results: a) UTS and b) elastic modulus.

5.8. Exponential model

Several values for the C and n coefficients of the proposed exponential model were also computed and optimized to reduce the overall prediction error of the exponential model. The results are shown in Table 9. The results predicted by the Exponential model and the experimental results are compared in Figure 10. From Figure 10a, it is observed that the proposed exponential model is able to predict with good accuracy the UTS experimental results. The maximum prediction errors are 17%, 29% and 36% for the flat, on-edge and up-right build orientations, respectively. It is worth mentioning that in the up-right orientation, the exponential model has a minimum error of 0% for infill values of 41% and 79%. In the case of the elastic modulus, Figure 10b, the maximum prediction errors are 19%, 58% and 48% for the flat, on-edge and up-right build orientations, respectively. Notice that this model does not predict accurately the mechanical behaviour of FDM parts with low infill values.

Table 9. Results of the C and n coefficients of the proposed exponential model.

Figure 10. Results of the exponential model vs. experimental results: a) UTS and b) elastic modulus.

6. Quantitative comparison and discussion

The prediction performance of the analytical models is now compared quantitatively for the three build orientations and the two mechanical properties. Table 10 summarizes the overall prediction errors and standard deviations of all models when predicting the UTS in the three build orientations. From this table it is observed that the model with the best prediction performance in the flat build orientation is the efficiency model (rank 1), with an average error of 0% and a standard deviation of 9.4%. In the on-edge and up-right build orientations, the Gibson & Ashby model has the best prediction performance (rank 1) with an average error of 0% and standard deviations of 14.1% and 14.8%, respectively. On the other hand, the rule of mixture model is the least accurate model (rank 8) in the three build orientations, with average errors of 16.4%, 11.6% and 206.3% in the flat, on-edge and up-right build orientations, respectively. This low performance is because this model assumes a linear structural behaviour proportional to the infill percentage for any build orientation, which is not appropriate for FDM parts.

Table 10. Summary of the models' average prediction errors for UTS.

Table 11 summarizes the overall prediction errors and standard deviations of all models when predicting the elastic modulus in the three build orientations. These results show that the best

prediction performance in the flat, on-edge and up-right build orientations is obtained with the Gibson & Ashby model (rank 1), followed by the efficiency model (rank 2) and the exponential model (rank 2). The worst prediction performance in the three build orientations was also obtained with the rule of mixture model (rank 8). Thus, it can be said that the Gibson & Ashby model is able to predict with good accuracy (low values of prediction errors) the elastic modulus behaviour of FDM components in any build orientation.

Table 11. Summary of the models' average prediction errors for the elastic modulus.

Table 12 presents a ranking of the analytical models based on their combined prediction performance in the three build orientations, i.e. considering the UTS and the elastic modulus. These results show that the efficiency model has the best prediction performance in the flat orientation, followed by the proposed exponential model and the Gibson & Ashby model. In the on-edge orientation, the Gibson & Ashby model led to the best performance, followed by the efficiency model and the proposed exponential model. In the up-right orientation, the best performance was also obtained by the Gibson & Ashby model, followed by the proposed exponential and variant Duckworth models. Table 12 also presents a global ranking of the models, which considers the prediction performance for the UTS and elastic modulus in the three build orientations. It is observed that the Gibson & Ashby model has the best global prediction performance followed by the efficiency and the new proposed exponential models. On the other hand, the worst performance was obtained by the rule of mixture since it only involves the infill percentage parameter.

Table 12. Ranking according to the build orientation and global performance.

In general, it can be said that the results obtained from the analytical models are congruent with the experimental results, giving a positive contribution to the study and understanding of the mechanical properties of parts manufactured by FDM. It has been demonstrated that analytical models are capable to predict with good accuracy the structural behaviour of FDM parts. Moreover, these models could be extended to other categories of similar AM parts.

7. Conclusions

An investigation to evaluate and compare several existing and new proposed analytical models tailored to predict the structural behaviour of FDM parts has been presented. The evaluation is based on comparing the ultimate tensile strength and the elastic modulus predicted by the analytical models, and the results obtained from experimental tensile tests on FDM specimens fabricated using variable process parameters. The results have revealed that some existing analytical models can be tailored to predict with good accuracy the mechanical behaviour of FDM parts. It was also observed that the most accurate model is the Gibson's & Ashby, followed by the efficiency model and the two new proposed exponential and variant Duckworth models. Thus, the use of analytical models to predict the structural behaviour of FDM parts, or categories of similar AM parts, based on the process parameters and material properties, is feasible. Consequently, analytical models can be used to assist the DfAM process, reducing the need of existing experimental and numerical approaches, which are time consuming and costly. Future work considers the evaluation of the analytical models using other materials and AM processes besides the FDM process.

Acknowledgments

The authors would like to thank the financial support from the National Science and Technology Council …

References

3D market, (2020), "3D market, impresoras 3d", available at: https://www.3dmarket.mx/ (accessed may 05, 2020).

ASTM International, (2014), "D638 Standard Test Method for Tensile Properties of Plastics", *ASTM International*, pp. 1-17.

Anh S.H., Montero M., Odell D., Roundy S. and Wright P.K., (2002), "Anisotropic material properties of fused deposition modelling ABS", *Rapid Prototyping Journal,* Vol. 8, pp. 248-257.

Alafaghani A., Qattawi A. and Ablat M.A., (2017), "Design Consideration for Additive Manufacturing: Fused Deposition Modelling", *Open Journal of Applied Sciences,* Vol. 7, pp. 291-318.

Ang K.C., Leong K.F., Chua C.K. and Chandrasekaran M., (2006), "Investigation of the mechanical properties and porosity relationships in fused deposition modelling-fabricated porous structures", *Rapid Prototyping Journal*, Vol. 12, pp. 100-105.

Casavola C., Cazzato A., Moramarco V. and Pappalettere C., (2016), "Orthotropic mechanical properties of fused deposition modelling parts described by classical laminate theory", *Materials and Design*, Vol. 90, pp. 453-458.

Cerda-Avila S.N., Medellin-Castillo H.I. and de Lange D.F., (2019), "Analysis and numerical simulation of the structural performance of Fused Deposition Modeling samples with variable infill values", *Journal of Engineering Materials and Technology*, Vol. 141(2), pp. 021005-021005-7.

Cerda-Avila Steffany N., Medellín-Castillo, Hugo Iván, Lim Theodore (2020), "An experimental methodology to analyse the structural behaviour of FDM parts with variable process parameters", *Rapid prototyping journal*, Vol. 26(9), pp. 1615-1625.

Chacón J.M., Caminero M.A., García-Plaza E. and Núñez P.J., (2017), "Additive manufacturing of PLA structures using fused deposition modelling: Effect of process parameters on mechanical properties and their optimal selection", *Materials & Design*, Vol. 124, pp. 143-157.

Choren J.A., Heinrich S.M. and Silver-Thorn M.B., (2013), "Young's modulus and volume porosity relationships for additive manufacturing aplications", *Journal of Materials Science*, Vol. 48, pp. 5103-5112.

Christensen R.M., (2000), "Mechanics of cellular and other low-density materials", *International Journal of Solids and Structures*, Vol. 37, pp. 93-104.

Color Plus, (2020), "Color Plus", available at: https://www.colorplus3d.com/ (accessed may 05, 2020).

Costa S.F., Duarte F.M. and Covas J.A., (2017), "Estimation on filament temperature and adhesion development in fused deposition techniques", *Journal of Materials Processing Technology*, Vol. 245, pp. 167-179.

Croccolo D., De Agostinis M. and Olmi G., (2013), "Experimental characterization and analytical modelling of the mechanical behavior of fused deposition processed parts made of ABS-M30", *Computational Materials Science*, Vol. 79, pp. 506-518.

Cuan-Urquizo E., Barocio E., Tejada-Ortigoza V., Pipes R.B., Rodriguez C.A. and Roman-Florrs A., (2019), "Characterization of the Mechanical Properties of FFF Structures and Materials: A Review on the Experimental, Computational and Theoretical Approaches", *Materials,* Vol. 12, pp. 1-25.

Domingo-Espin M., Puigoriol-Forcada J.M., Garcia-Granada A.M., Lluma J., Borros S. and Reyes G., (2015), "Mechanical property characterization and simulation of fused desposition modeling Polycarbonate parts", *Materials & Design*, Vol. 83, pp. 670-677.

Gallegos-Nieto E., Medellín-Castillo H.I. and de Lange D.F., (2015), "A complete structural performance analysis and modelling of hydroxyapatite scaffolds with variable porosity", *Computer Methods in Biomechanics and Biomedical Engineering*, Vol. 18, pp. 1225-1237.

Garg A., Tai K., Lee C.H. and Savalani M.M., (2014), "A hybrid M5'-genetic programming approach for ensuring greater trustworthiness of prediction ability in modelling of FDM process", *Journal of Intelligent Manufacturing*, Vol. 25, pp. 1349-1365.

Gibson L. and Ashby M.F., (1988), "Cellular solids: structure and properties", *Oxford: Pergamon Press.*

Górski F., Kuczko W., Wichniarek R. and Hamrol A., (2015), "Computation of Mechanical Properties of Parts Manufactured by Fused Deposition Modeling Using Finite Element Method", *Advances in Intelligent Systems and Computing*, Vol. 368, pp. 403-413.

Hambali R.H., Celik H.K., Smith P.C. and Rennie A., (2010), "Effect of Build Orientation of FDM parts: a Case Study for Validation of Deformation Behaviour by FEA", *IDECON 2010-International Conference on Design and Concurrent Engineering*, pp. 224-228.

Hernández-Rivera J.L., Medellín-Castillo H.I. and de Lange D.F., (2016), "Numerical and theoretical modeling of the elasto-plastic response of aluminum-graphite composites during straining", *Materials Science & Engineering A*, Vol. 650, pp. 323-334.

Mouhmid B., Imad A., Benseddiq N., Benmedakhene S. and Maazouz A., (2006), "A study of the mechanical behavior of a glass fibre reinforced polyamide 6,6: Experimental investigation", *Polymer Testing*, Vol. 25, pp. 544-552.

Panda B., Leite M., Biswal B.B., Niu X. and Garg A., (2018), "Experimental and numerical modelling of mechanical properties of 3D printed honeycomb structures", *Measurement*, Vol. 116, pp. 495-506.

Rayegani F. and Onwubolu G.C., (2014), "Fused deposition modelling (FDM) process parameter prediction and optimization using group method for data handling (GMDH) and differential evolution (DE)", *The International Journal of Advanced Manufacturing Technology*, Vol. 73, pp. 509-519.

Rezayat H., Zhou W., Siriruk A., Penumadu D. and Babu S.S., (2015), "Structure-mechanical property relationship in fused deposition modelling", *Materials Science and Technology*, Vol. 31:8, pp. 895-903.

Roberts A.P. and Garbozzi E.J., (2002), "Computation of the linear elastic properties of random porous materials with a wide variety of microstructure", *Proceedings of the Royal Society A*, Vol. 458, pp. 1033-1054.

Sealy M.P., Kanger C., Hadidi H., Akula C., Sandman C., Quint J., Alsunni M., Underwood R., Slafter C., Sonderup J., Spilinek M., Casias J. and Rao P., (2017), "Effect of Process Parameters and Shot Peening on Mechanical Behavior ob ABS Parts Mnaufactured by Fused Filament Fabrication (FFF)", Solid Freeform Fabrication 2017: Proceedings of the 28th Annual International Solid Freeform Fabrication Symposium – An Additive Manufacturing Conference, pp. 444-458.

Somireddy M. and Czekanski A., (2017), "Mechanical characterization of Additively Manufactured Parts by FE Modeling of Mesostructure", *Journal of Manufacturing and Materials Processing,* Vol. 1(2), pp. 1-21.

Somireddy M., Czekanski A. and Singh C.V., (2018), "Development of constitutive material model of 3D printed structure via FDM", *Materials Today Communications,* Vol. 15, pp. 143-152.

Sukindar N.A.B., Ariffin M., Baharudin B., Jaafar C. and Ismail M., (2017), "Analysis on the Impact Process Parameters on Tensile Strength Using 3d Printer Repetier-Host Software", *ARPN Journal of Engineering and Applied Science,* Vol. 12, pp. 3341-3346.

Vanaei H., Shirinbayan M., Deligant M., Raissi K., Fitoussi J., Khelladi S., and Tcharkhtchi A., (2020), "Influence of process parameters on thermal and mechanical properties of polylactic acid fabricated by fused filament fabrication", *Polymer Engineering & Science,* Vol. 60(8), pp. 1822-1831.

Wang Y. and Huang Z., (2018), "Analytical Micromechanics Models for Elastoplastic Behavior of Long Fibrous Composites: A Critical Review and Comparative Study", *Materials*, Vol. 11(10), pp. 1919.

Zhang Y. and Chou Y.K., (2006), "Three- dimensional finite element analysis simulations of the fused deposition modelling process", *Proceedings of the Institution of Mechanical Engineers, Part B: Journal of Engineering Manufacture*, Vol. 220, pp. 1663–1671.

Table 1. FDM process parameters used in the fabrication of the test specimens.

Process parameter	Values	Units
Nominal infill percentage	5, 10, 20, 40, 80, 100	%
Perimeter layers	1, 2	-
Build orientation	flat, on-edge, up-right	-
Upper/bottom layers	2, 3	-
Layer thickness	0.14, 0.18, 0.30	mm
Raster angle	±45, 0/90	°
Deposition speed	80	mm/s
Extrusion temperature	200	°C

Table 2. Characteristics of the PLA filaments.

PLA filament characteristics	Values	Units
Diameter	1.75	mm
Tensile strength	55 - 65	MPa
Density	1.24	g/cm^3
Extruder temperature	190 - 220	°C
Bed temperature	45 – 60	°C

Table 3. Values of the α coefficient.

Property	Build orientation		
	Flat	On-edge	Up-right
UTS	0.8592	0.8958	0.3264
Elastic modulus	0.7053	0.683	0.4557

Table 4. Values of the *C* and *n* coefficients.

Property	Coefficient	Build orientation		
		Flat	On-edge	Up-right
UTS	***n***	0.8951	1.072	1.6456
	C	0.8037	0.9272	0.4583
Elastic modulus	***n***	1.028	1.2278	1.3326
	C	0.7175	0.7671	0.5456

Table 5. Values of the *k* and *m* coefficients.

Coefficient (property)	Build orientation		
	Flat	On-edge	Up-right
***k* (UTS)**	1.9426	1.8605	6.5850
***m* (elastic modulus)**	2.4810	2.7690	4.6260

Table 6. Values of the *r* coefficient.

Property	Build orientation		
	Flat	On-edge	Up-right
UTS	1.1830	1.3405	0.3638
Elastic modulus	0.9074	0.8940	0.5354

Table 7. Values of the *A* coefficient.

Property	Build orientation		
	Flat	On-edge	Up-right
UTS	-1.4400	-1.3881	-14.8250
Elastic modulus	-2.2350	-2.7515	-7.4400

Table 8. Values of the β and m coefficients.

Property	Coefficient	Build orientation		
		Flat	On-edge	Up-right
UTS	m	1.9550	1.7050	2.6141
	β	1.0208	0.9512	0.4704
Elastic modulus	m	1.7571	1.9355	3.4445
	β	0.7610	0.7767	0.8033

Table 9. Results of the C and n coefficients of the proposed exponential model.

Property	Coefficient	Build orientation		
		Flat	On-edge	Up-right
UTS	n	1.9235	1.7050	2.9477
	C	0.1450	0.1729	0.0268
Elastic modulus	n	1.8774	1.8870	2.6435
	C	0.1221	0.1158	0.0457

Table 10. Summary of the models' average prediction errors for UTS.

Models	Build orientation								
	Flat			On-edge			Up-right		
	Average error (%)	Std. dev. (%)	Rank	Average error (%)	Std. dev. (%)	Rank	Average error (%)	Std. dev. (%)	Rank
Rule of mixture	16.4	11.0	8	11.6	16.0	8	206.3	116.4	8
Efficiency	0.0	9.4	1	0.0	14.4	2	0.0	38.0	4
Gibson & Ashby	0.0	11.8	6	0.0	14.1	1	0.0	14.8	1
Duckworth	0.0	10.5	5	0.0	17.0	4	0.0	83.8	7
Rice	0.0	20.3	7	0.0	21.0	7	0.0	43.4	5
Hasselman	-0.1	10.4	3	0.0	17.5	6	0.0	74.1	6
Variant Duckworth*	0.0	10.4	4	0.0	17.2	5	0.0	23.5	3
Exponential*	0.0	9.9	2	0.0	16.1	3	-1.4	19.3	2

* Proposed model

Table 11. Summary of the models' average prediction errors for the elastic modulus.

Models	Build orientation								
	Flat			On-edge			Up-right		
	Average error (%)	Std. dev. (%)	Rank	Average error (%)	Std. dev. (%)	Rank	Average error (%)	Std. dev. (%)	Rank
Rule of mixture	41.8	8.2	8	46.4	28.9	8	119.4	80.4	8
Efficiency	0.0	5.8	2	0.0	19.8	2	0.0	36.6	4
Gibson & Ashby	0.0	4.9	1	0.0	14.1	1	0.0	18.7	1
Spriggs	0.0	19.4	6	0.0	29.6	7	0.0	60.8	7
Rice	0.0	15.4	5	0.0	29.4	6	0.0	44.7	5
Hasselman	0.0	22.1	7	0.0	28.8	5	0.0	55.2	6
Variant Duckworth*	0.0	11.7	4	0.0	25.4	4	0.0	35.2	3
Exponential*	-0.1	9.8	3	0.0	24.4	3	0.0	26.8	2

* Proposed model

Table 12. Ranking according to the build orientation and global performance.

Models	Rank			
	Build orientation			Global
	Flat	On-edge	Up-right	
Gibson & Ashby	3	1	1	1
Efficiency	1	2	4	2
Exponential*	2	3	2	2
Variant Duckworth*	5	4	3	3
Hasselman	4	5	6	4
Rice	6	6	5	5
Duckworth	5	5	7	6
Rule of mixture	7	7	8	7

* Proposed model

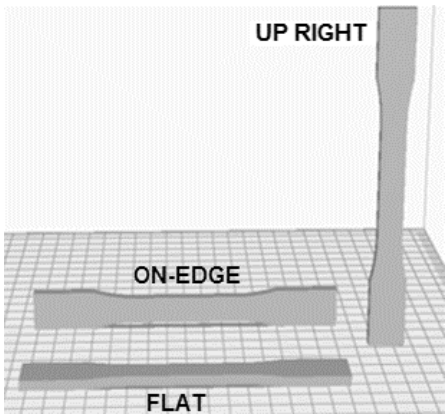

Figure 1. Schematic representation of the build orientation FDM process parameter.

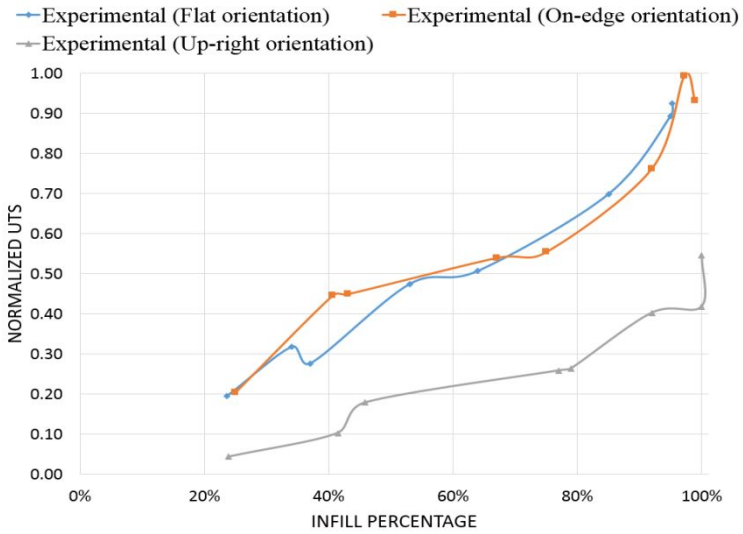

a)

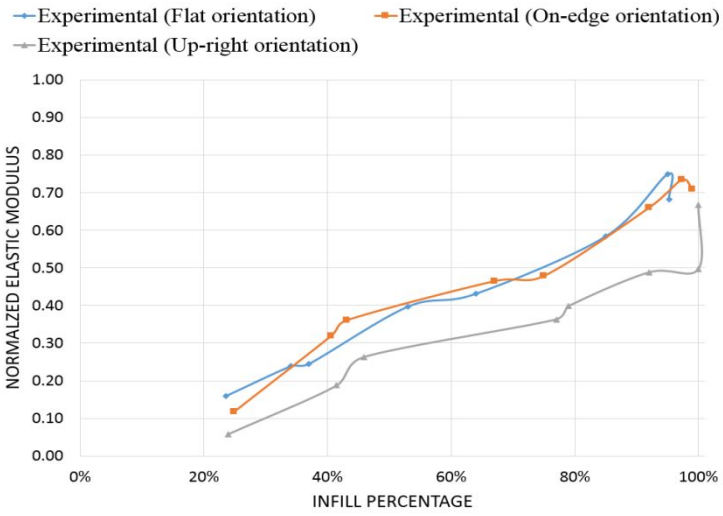

b)

Figure 2. Experimental results for: a) UTS, b) elastic modulus.

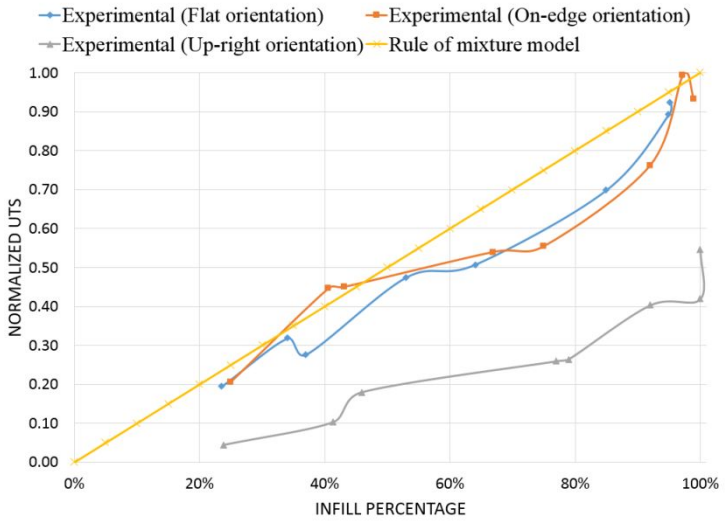

a)

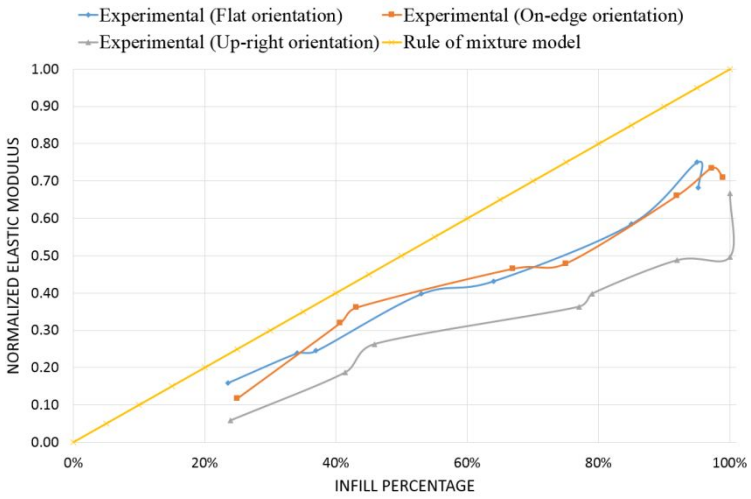

b)

Figure 3. Results of the rule of mixture model vs. experimental results: a) UTS and b) elastic modulus.

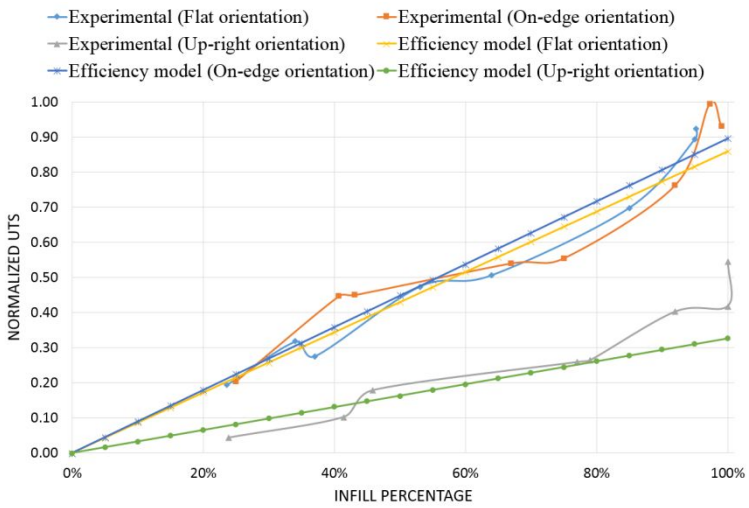

a)

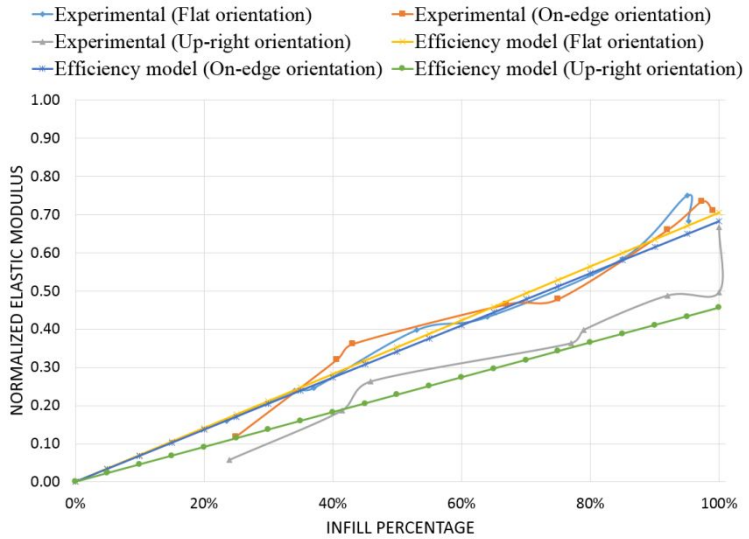

b)

Figure 4. Results of the Efficiency model vs. experimental results: a) UTS and b) elastic modulus.

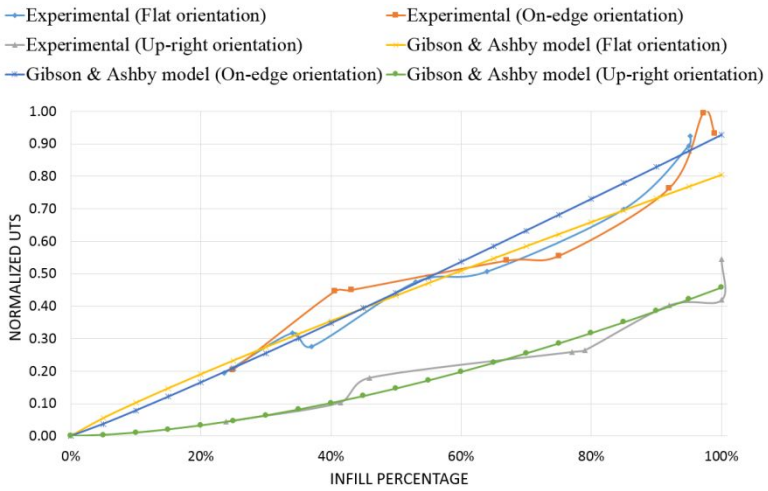

a)

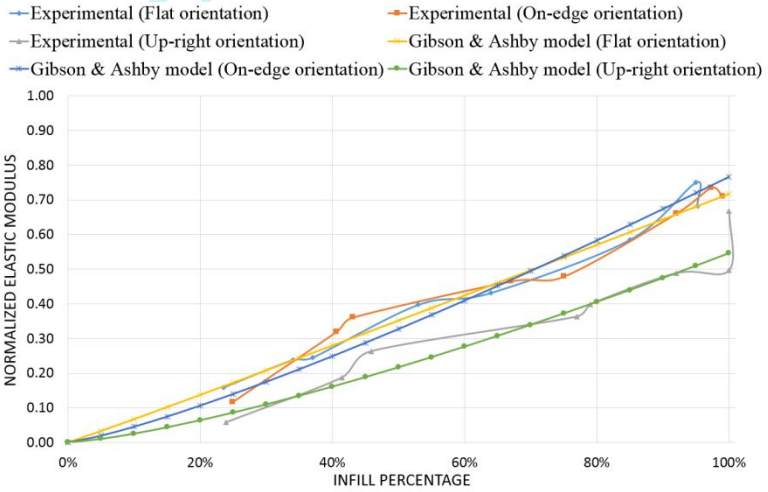

b)

Figure 5. Results of the Gibson & Ashby model vs. experimental results: a) UTS and b) elastic modulus.

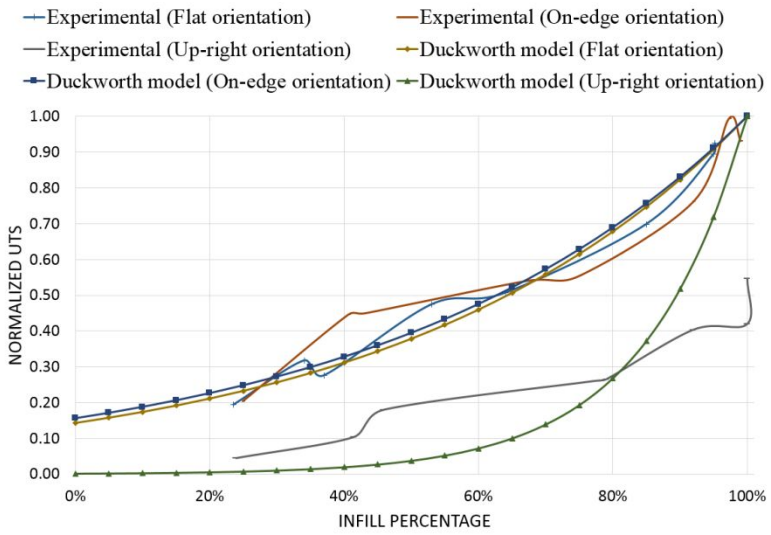

a)

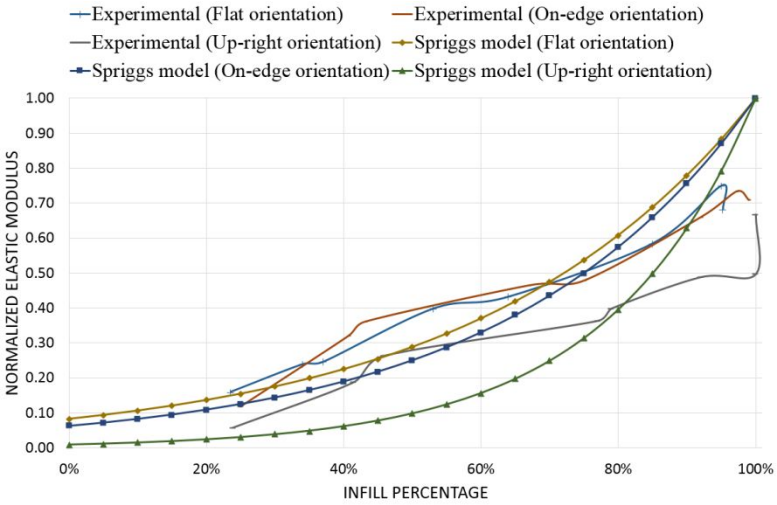

b)

Figure 6. Results of the Duckworth and Spriggs models vs. experimental results: a) UTS (Duckworth) and b) elastic modulus (Spriggs).

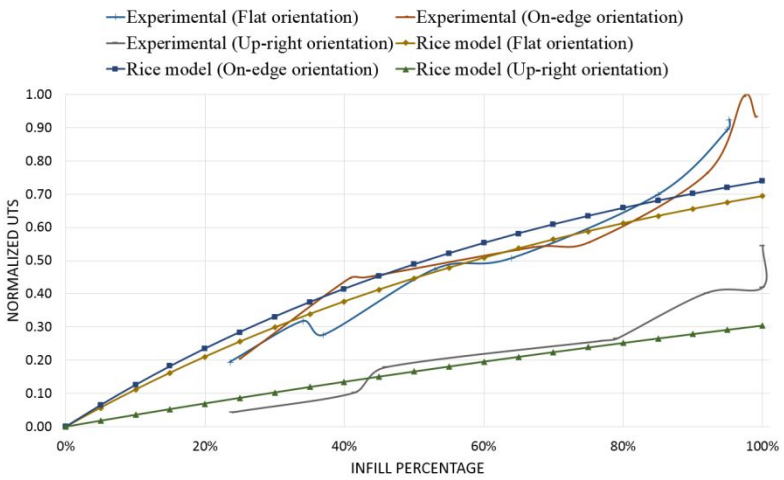

a)

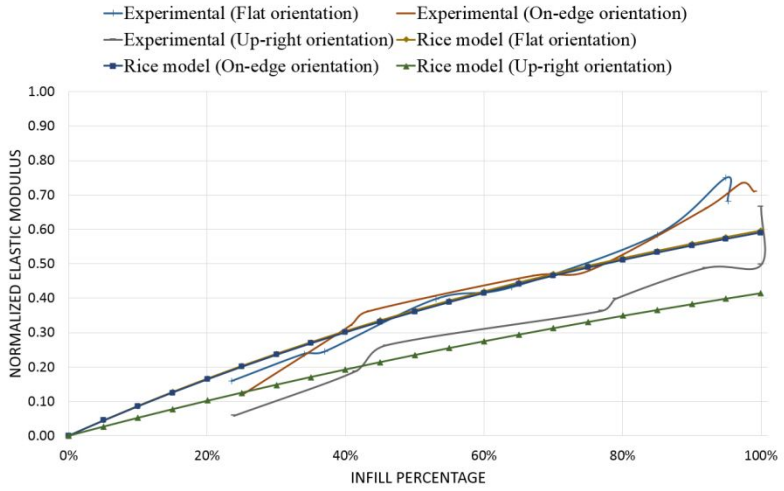

b)

Figure 7. Results of the Rice model vs. experimental results: a) UTS and b) elastic modulus.

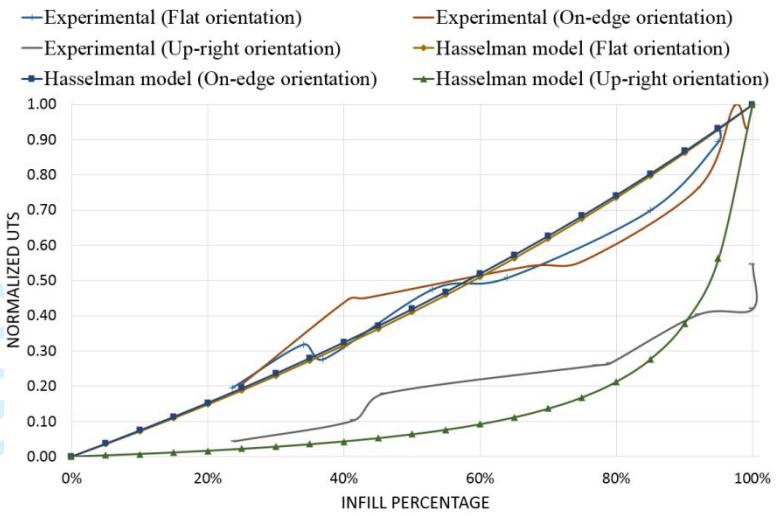

a)

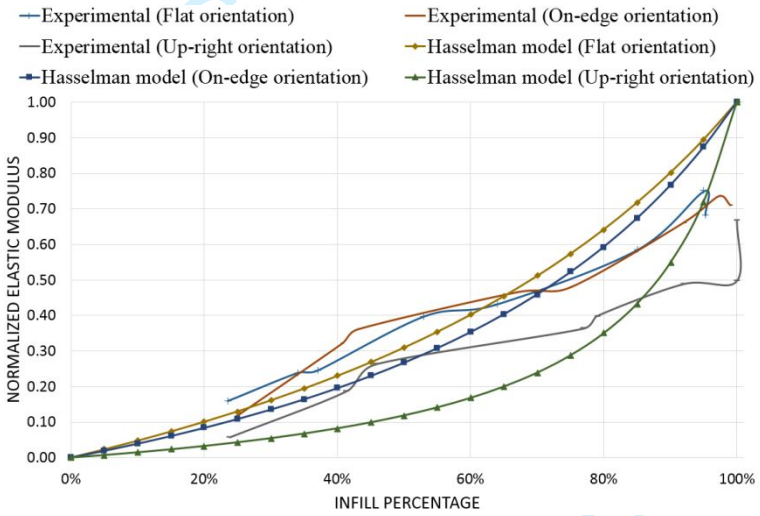

b)

Figure 8. Results of the Hasselman model vs. experimental results: a) UTS and b) elastic modulus.

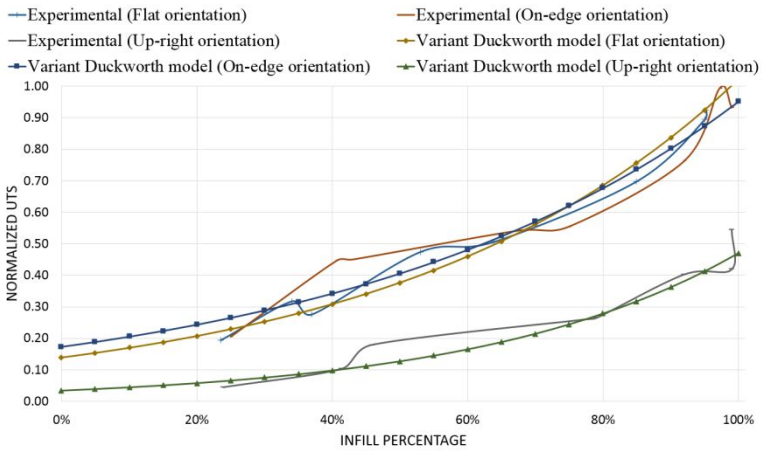

a)

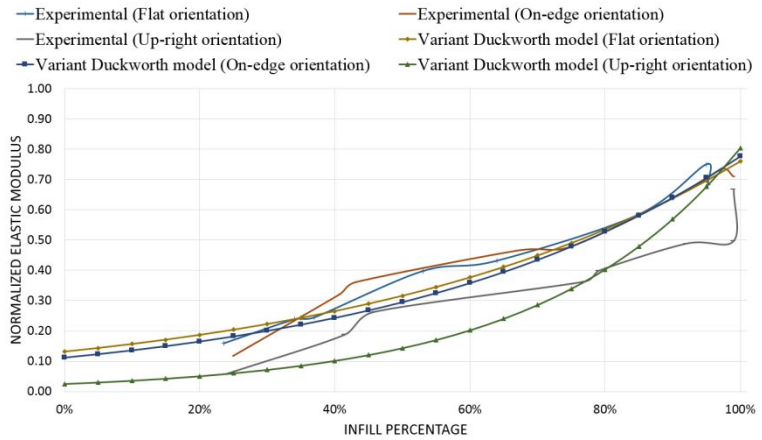

b)

Figure 9. Results of the Variant Duckworth model vs. experimental results: a) UTS and b) elastic modulus.

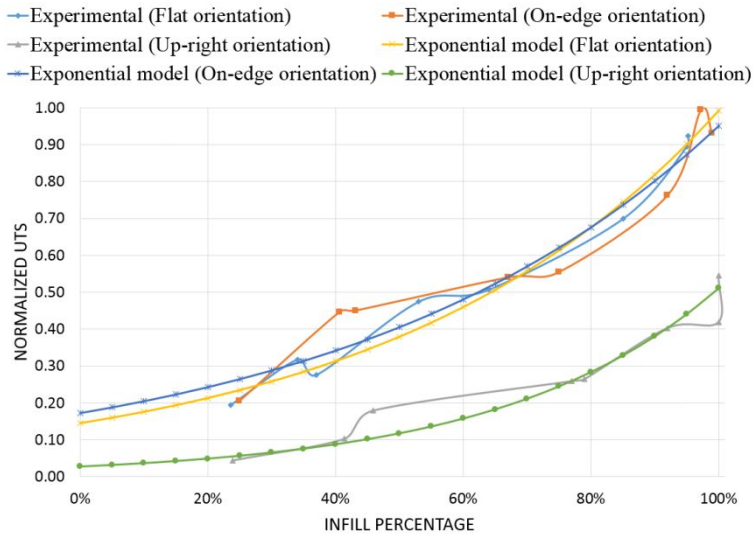

a)

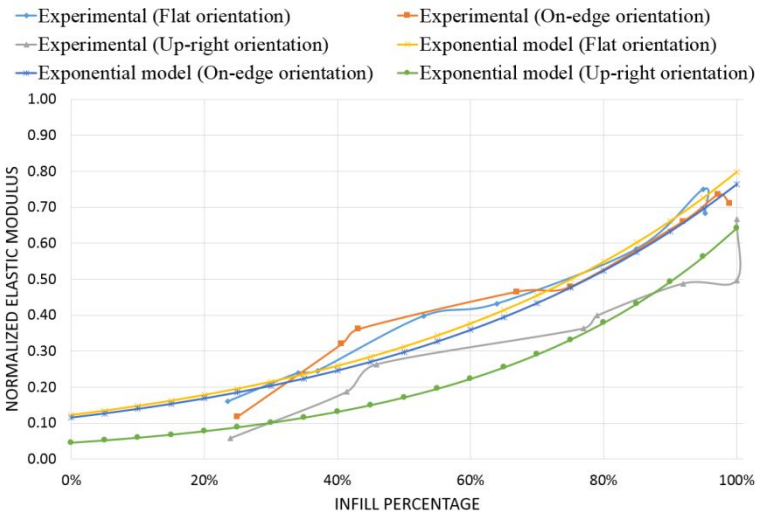

b)

Figure 10. Results of the exponential model vs. experimental results: a) UTS and b) elastic modulus.